

# <sup>1</sup> Context-dependent consequences of lagged effects in demographic <sup>2</sup> models

<sup>3</sup> Eric R. Scott<sup>1,5</sup>, María Uriarte<sup>2</sup>, Emilio M. Bruna<sup>1,3,4</sup>

<sup>4</sup> <sup>1</sup>Department of Wildlife Ecology and Conservation, University of Florida, Gainesville, Florida 32611-0430  
<sup>5</sup> USA

<sup>6</sup> <sup>2</sup>Department of Ecology, Evolution and Environmental Biology, Columbia University 1200 Amsterdam  
<sup>7</sup> Avenue, New York, New York 10027 USA

<sup>8</sup> <sup>3</sup>Center for Latin American Studies, University of Florida, Gainesville, Florida 32611-5530 USA

<sup>9</sup> Biological Dynamics of Forest Fragments Project, INPA-PDBFF, CP 478, Manaus, Amazonas 69011-970  
<sup>10</sup> Brazil

<sup>5</sup>Current Address: CCT Data Science, University of Arizona, Tucson, AZ 85721 USA

12 (draft: 11 February 2026)

13

## Abstract

14 Text of 150 words max summarizing this amazing paper.

15 **Keywords:** demography, environmental stochasticity, integral projection models, lagged effects,

16 structured population models, population dynamics

17 **Manuscript elements:** Figures 1-4, Tables 1-6

18 **Manuscript type:** e-note

19

## Introduction

20 Current environmental conditions can have immediate effects on the growth, survival, or reproduction of  
 21 long-lived organisms. However, there is mounting evidence for potential delays of months or even years  
 22 between current environmental conditions and resulting changes in demographic vital rates. These *Lagged*  
 23 *Effects*, also known as *Delayed Life-history Events* (i.e. DLHEs, Beckerman et al. 2002), can  
 24 simultaneously affect an entire cohort (e.g., all juveniles hatching during a period of scarcity will have  
 25 delayed maturation) or only a subset of the population (e.g., a freeze reduces flowering by small trees but  
 26 not large ones). Moreover, the temporal delay between an environmental event and the resulting changes in  
 27 demographic vital rates may depend on both the intensity of the event and its timing relative to the  
 28 underlying physiological mechanisms (Criley and Lekawatana 1994; Evers et al. 2021). For example, a  
 29 drought during the early stages of gestation or floral bud formation might have a much larger impact on  
 30 the number of offspring or fruits produced than one at a later stage. The delay or intensity of lagged effects  
 31 could also be location-specific – individuals in some sites or habitats could be buffered against or able to  
 32 recover more quickly from the delayed effects of environmental variation.

33 Because Lagged Effects are often directly linked to reproduction and survival, it has been argued they  
 34 could have major but underappreciated consequences for population dynamics (Beckerman et al. 2002).  
 35 While recent studies suggest this could indeed be the case (e.g., Williams et al. 2015; Molowny-Horas et al.  
 36 2017; Tenhumberg et al. 2018), there have been few efforts to test this hypothesis (Metcalf et al. 2015).  
 37 This is partly because experimental tests of lagged effects are challenging to design, implement, and  
 38 maintain (Kuss et al. 2008). While observational data can also be used to detect lagged effects, doing so  
 39 requires long-term data on both the potential lagged effects and its hypothesized environmental drivers.  
 40 Not only are such coupled data sets extremely rare (*sensu* Evers et al. 2021), the tools for both identifying  
 41 lagged effects and modeling their demographic impacts can be challenging to implement. For example,  
 42 many of the potentially applicable statistical methods have stringent assumptions and data requirements  
 43 rarely met by ecological data (Metcalf et al. 2015). Terms for complex biological processes such as lagged  
 44 effects can also render demographic models less tractable or amenable to analysis using currently available  
 45 tools. Addressing these challenges is a major undertaking, the value of which depends on the effort  
 46 required to consider lagged effects vs. the potential consequences of failing to do so — consequences that  
 47 could include overestimating projections of population growth rate (i.e.,  $\lambda$ ) in a conservation setting to  
 48 drawing invalid conclusions regarding support for the predictions of ecological or evolutionary theory.

49 Integral Projection Models (i.e., IPMs) are an important and widely used tool for studying  
 50 demography and population dynamics (Ellner and Rees 2006; Rees and Ellner 2009; Rees et al. 2014).

51 Their flexibility, in concert with a rapidly growing suite of software, data, and other resources  
52 (Salguero-Gómez et al. 2015; Ellner et al. 2016; Levin et al. 2021), have facilitated their use to study a  
53 wide range of topics in ecology, evolution, and conservation (Morris and Doak 2002; Crone et al. 2011;  
54 Ellner et al. 2016). Mathematical and statistical advances (e.g., Williams et al. 2012; Brooks et al. 2019)  
55 have rapidly expanded the scope of questions and biological processes that can be investigated with these  
56 models (e.g., Metcalf et al. 2015; Ellner et al. 2016; Rees and Ellner 2016). Here we investigate if including  
57 lagged effects in Integral Projection Models alters projections of  $\lambda$  and population structure, and how these  
58 projections are influenced by habitat-specific differences in lag length and magnitude.

59 We have previously shown that the effects of precipitation extremes on the demographic vital rates of  
60 an Amazonian understory herb (*Heliconia acuminata*, Heliconiaceae) can be delayed up to 36 months  
61 (Scott et al. 2022), with the presence and duration of these lagged effects varying by vital rate. We also  
62 showed that the magnitude and lagged effects differs by habitat - lagged effects on survival and growth  
63 were far more pronounced for plant populations in isolated forest fragments than for those in continuous  
64 primary forest. Here we parameterize three classes of Integral Projection Models — a deterministic IPM, a  
65 stochastic IPM, and a stochastic IPM with lagged effects of precipitation on vital rates — using data from  
66 populations in either Continuous Forest or Forest Fragments. We then used these models to address two  
67 questions: First, how similar are the projections of  $\lambda$  from stochastic IPMs with and without lagged effects?  
68 Second, do habitat-specific differences in lagged effects translate into habitat-specific projections of  $\lambda$ ?

## 69 Methods

### 70 Study System and Demographic Data

71 *Heliconia acuminata* (Heliconiaceae) is a perennial, self-incompatible monocot that is distributed  
72 throughout much of the Amazon basin (Kress 1990). While some *Heliconia* species grow in large  
73 aggregations on roadsides, gaps, and in other disturbed habitats, others, including *H. acuminata*, grow  
74 primarily in the forest understory (Kress 1983; Ribeiro et al. 2010). Understory *Heliconia* species produce  
75 fewer flowers and are pollinated by traplining hummingbirds (Stouffer and Bierregaard 1996; Bruna et al.  
76 2004). The models and analyses here are based on 11 years (1998-2009) of demographic data collected on  
77 >8500 *H. acuminata* found at Brazil's Biological Dynamics of Forest Fragments Project (BDFFP), located  
78 ~70 km north of Manaus, Brazil. The BDFFP reserves include both continuous forest and forest fragments  
79 that range in size from 1-100 ha. These fragment reserves were originally isolated in the early 1980's by the  
80 creation of cattle pastures, with the secondary growth surrounding them periodically cleared to ensure  
81 their continued isolation. The habitat in all sites is non-flooded lowland rain forest with rugged

82 topography. A complete summary of the BDFFP and its history can be found in Bierregaard et al. (2001).

83 A complete description of our demographic methods, data, and analyses to date can be found in

84 Bruna et al. (2023). Briefly, in 1997–1998 a series of 5000 m<sup>2</sup> plots were established in the BDFFP

85 reserves: N=6 in Continuous Forest and N=4 in 1-ha Forest Fragments (i.e., CF and FF, respectively). All

86 of the *Heliconia acuminata* in these plots were marked and measured; the plots were censused annually, at

87 which time a team recorded the size of surviving individuals, marked and measured new seedlings, and

88 identified any previously marked plants that died. Each plot was also surveyed 4-5 times during the

89 flowering season to identify reproductive plants. These surveys were complemented by data on the number

90 of fruits per flowering plant (Bruna 2021) and seeds per fruit (Bruna 2014) that were collected outside of

91 the demographic plots to avoid altering within-plot recruitment. We also conducted experiments to

92 quantify the probability of seed germination and seedling establishment in both forest fragments and

93 continuous forest (Bruna 1999, 2002).

94 The rainy season in our sites is typically from late December through late May. *Heliconia acuminata*

95 in our site begin flowering early in the rainy season and most reproductive plants produce a single

96 inflorescence (range = 1–7) with 20–25 flowers (Bruna and Kress 2002). Fruits mature April-May and have

97 1–3 seeds per fruit ( $\bar{x} = 2$ ) that are dispersed by a thrush and several species of manakin (Uriarte et al.

98 2011). Dispersed seeds germinate approximately 6 months after dispersal at the onset of the subsequent

99 rainy season, with rates of germination and seedling establishment higher in continuous forest than forest

100 fragments (Bruna 1999, 2002). The median number of plants in CF plots was over twice that of the plots

101 in 1-ha fragments (CF: median = 788, range = 201-1549; 1-ha: median = 339, range = 297-400, Bruna et

102 al. (2023)).

### 103 ***Construction of Integral Projection Models***

104 We projected the growth rate and structure of *Heliconia acuminata* with three classes of IPMs: (1)

105 deterministic, (2) stochastic, and (3) stochastic with lagged environmental effects. Each of these IPMs

106 required different functional forms of the underlying vital rate functions used to describe the *H. acuminata*

107 life cycle (Figure 1). All models were density-independent, with the deterministic model serving as the

108 foundation for the more complex models. Our modeling workflows were managed using the **targets** R

109 package (Landau 2021); in addition to ensuring reproducibility this allowed us to track computational time

110 spent processing and analyzing each class of IPM.

111 **(1) Deterministic IPM:** In this model the size and structure of a population in year  $t + 1$  is

112 determined by the survival and change in size of the  $n$  plants of size  $z$  that are alive in year  $t$  (Equation 1)

113 plus the number of new seedlings that entered the population (Equation 2):

$$n(z', t + 1) = \int_L^U P(z', z)n(z, t) dz + R(z')n_s(t) \quad (1)$$

$$n_s(t + 1) = \int_L^U F(z)n(z, t) dz \quad (2)$$

114 Equation 1 has two components. The first is sub-kernel  $P(z', z)$ , which describes the size-dependent  
115 probability of survival of mature (i.e., post-seedling) plants,  $s$ , and their growth (or regression) from size  $z$   
116 to  $z'$ :

$$P(z', z) = s(z)G(z', z) \quad (3)$$

117 The second component is sub-kernel  $R(z')$ . This sub-kernel describes the survival of seedlings to year  $t + 1$   
118 of seedlings that established in year  $t$  and the size of these surviving seedlings when they transition into the  
119 ‘mature’ plant population after surviving one year:

$$R(z') = s_s G_s(z') \quad (4)$$

120 Note that in Equation 4 both the probability that newly established seedlings survive their first year,  $s_s$ ,  
121 and the size to which they grow at the end of this year,  $G_s$ , are size-independent. IPMs can readily  
122 accommodate such transitions of individuals from a discrete state to a continuous one (i.e., from ‘seedling’  
123 to ‘mature plant of size  $z'$ ’; Ellner et al. 2016); we treated seedlings as a distinct and discrete category in  
124 our models because they have lower survival and growth in their first year than comparably sized but  
125 plants that have been established for over one year (Bruna 2003; Scott et al. 2022).

126 The number of new seedlings entering the population in year  $t + 1$  is a function of the number of  
127 ‘mature’ plants in year  $t$  and a sub-kernel describing the fecundity of these individuals:

$$F(z) = p_f(z)f(z)g \quad (5)$$

128 In this sub-kernel both the probability that a mature plant will flower,  $p_f$ , and the number of seeds a  
129 flowering plant will produce,  $f$ , are size-dependent, but all seeds germinate and establish as seedlings with  
130 probability  $g$ .

131 We used the annual census data (Bruna 2003) to fit the deterministic vital rate functions for growth,  
132 survival, and flowering in each habitat type (Table 1). The data from all plots within a habitat class were

133 pooled to create a single ‘summary population’ representing that habitat type; the summary populations  
134 were then used to fit the vital rate functions. A summary population is a superior means of synthesizing  
135 the demography of multiple populations than calculating an average vital rate for multiple populations  
136 because it corrects for the disproportionate weight that the low plant numbers in some size classes in some  
137 locations can give to vital rates (Caswell 2001; Bruna 2003). For established plants the vital rates were  
138 modeled as a smooth function of size in the previous census with generalized additive models (GAMs) fit  
139 with the `mgcv` package (Wood 2011) for the R statistical programming language (R Core Team 2020). For  
140 consistency, seedling survival and growth were also modeled using GAMs, but without size in the previous  
141 census as a predictor (i.e. ‘intercept-only’ models). For growth models a scaled t family distribution  
142 provided a better fit to the data than a Gaussian fit, as the residuals with a simple Gaussian model were  
143 leptokurtic. To model size-specific fecundity we used the data on fruits per flowering plant (Bruna 2021),  
144 seeds per fruit (Bruna 2014), and experimentally derived estimates of seed germination and seedling  
145 establishment (Bruna 1999, 2002).

146       **(2) Stochastic IPMs:** To include temporal stochasticity in our IPMs we included a random effect of  
147 year. This was done using a factor-smooth interaction that allowed the functional form of the relationship  
148 between plant size and vital rates to vary among transition years (Figure 1). We generated kernels for  
149 every transition year using the long-term survey data (Bruna et al. 2023) and random smooths for year.  
150 We then randomly selected one of these sets of kernels to use in each iteration of the IPM. This procedure  
151 is equivalent to ‘kernel resampling’ (*sensu* Metcalf et al. 2015) or matrix selection for matrix population  
152 models (Caswell 2001; Boyce et al. 2006).

153       **(3) Stochastic IPMs with lagged effects of precipitation on vital rates:** We explicitly  
154 modeled the lagged effects of precipitation extremes on vital rates using the procedure described in Scott et  
155 al. (2022). Briefly, we first calculated the Standardized Precipitation Evapotranspiraton Index (i.e., SPEI)  
156 for our study site using a published gridded dataset based on ground measurements (Xavier et al. 2016).  
157 After we fit vital rate models using the long-term survey data (Figure 1), we modeled delayed effects of  
158 SPEI with Distributed Lag Non-linear Models (i.e., DLNMs) with a maximum lag of 36 months (Scott et  
159 al. 2022). To iterate these parameter-resampled IPMs (*sensu* Metcalf et al. 2015) we first created a random  
160 sequence of SPEI values by sampling years of the observed (monthly) SPEI data. For every year we then  
161 calculated a lag of 36 months from the month in which that year’s census was completed. These values  
162 were then used to predict the fitted values from vital rate models, which generated different kernels for each  
163 iteration of the IPM. The kernels of successive iterations are not entirely independent — the SPEI values  
164 used to calculate vital rates include values used in the previous two iterations — but they are ergodic.

165 All IPMs were constructed and iterated using the `ipmr` package (Levin et al. 2021) for the R  
166 statistical programming language (R Core Team 2020). The IPMs used 100 meshpoints and the midpoint  
167 rule for calculating kernels (Rees et al. 2014). For each type of IPM we iterated the model for 1000 time  
168 steps, but discarded the first 100 time steps to omit transient effects. Stochastic growth rates ( $\lambda_s$ ) were  
169 calculated as the average  $\ln(\lambda)$  from each time step (Caswell 2001) and then back-transformed to allow for  
170 direct comparison with projections of  $\lambda$  from deterministic models. The initial starting vector primarily  
171 influences a population's transient dynamics; we therefore used the distribution of established plant sizes  
172 and proportion of seedlings in the full demographic data set as the initial population vector for all models.

173 Finally, we estimated the 95% confidence intervals for each IPMs projections of  $\lambda$ . To do so we first  
174 created 500 populations for each habitat type by sampling individual plants with replacement (i.e.,  
175 bootstrapping) until the population size of each matched that of the initial population vector. We then  
176 re-fit the vital rate models for growth, survival, and flowering for each of these bootstrapped population  
177 and constructed new IPMs for each population as above (the models for germination and establishment  
178 rate, fruits per flowering plant, and seeds per fruit were not refit because these were estimated using  
179 different data sets). The projections of  $\lambda$  for the new populations were then used to estimate the upper and  
180 lower 95% bias-corrected percentile intervals (Caswell 2001; Manly 2018).

181 **Statistical analyses**

182 **Comparison of  $\lambda$  in Continuous Forest and Forest Fragments**

183 To determine if the deterministic projections of  $\lambda$  for the populations in Continuous Forest (i.e.,  $\lambda^{CF}$ ) and  
184 Forest Fragments (i.e.,  $\lambda^{FF}$ ) were significantly different we used the randomization test procedure  
185 described by Caswell (2001). Briefly, we randomly assigned plants with their demographic history among  
186 two populations,  $R_1$  and  $R_2$ , that were equal in size to the original CF and FF populations. We then  
187 calculated  $\lambda^{R_1}$ ,  $\lambda^{R_2}$ , and the absolute value of the difference between the two (i.e.,  $\theta$ ). This was repeated N  
188 = 1000 times, after which we determined the proportion of simulations in which  $\theta$  was greater than the  
189 observed difference between  $\lambda^{CF}$  and  $\lambda^{FF}$  (i.e.,  $P[\theta \geq \theta_{obs}]$ ).

190 We used a Generalized Linear Model to compare the projections of  $\lambda$  from the stochastic IPMs with  
191 and without lagged effects. We modeled  $\lambda_i$  as a function of IPM type (i.e., with and without lagged effects)  
192 and habitat (i.e., continuous forest vs. fragments), and the interaction of IPM type and habitat. Because  
193 the response variable ( $\lambda$ ) was continuous we used the Gaussian distribution with the identity link function  
194 in our model. We verified the model assumptions by plotting residuals versus fitted values.

195 **Population Structure**

196 Finally, we compared the structure of populations that were projected through the first 250 time steps in  
197 each habitat by the IPMs with and without lagged effects. At each time step, we assigned the individuals  
198 to one of four stage classes based on plant size, probability of survival, and probability of reproduction (see  
199 Table 2). We then calculated the proportion of the population that was in each stage class in each habitat  
200 for each IPM type. Comparing the means and variances of these proportions will allow us to determine (1)  
201 if the two IPMs project different population structures over time, (2) if the population structure for a given  
202 IPM is consistent across habitat type. Because Shapiro-Wilk tests indicated that the distributions of  
203 proportions were not normally distributed, we used the non-parametric Ansari-Bradley Test to compare  
204 the distribution of proportions in each habitat x stage combination. These analyses were conducted using  
205 the R packages `rstatix` and `vartest`, respectively (Kassambara 2023; Cosar and Dag 2024).

206 **Results & Discussion**

207 All IPMs projected higher population growth rates for *Heliconia acuminata* populations in Continuous  
208 Forest than for those in Forest Fragments (Table 3). The differences between  $\lambda^{CF}$  and  $\lambda^{FF}$ , which ranged  
209 from 1.19-2%, were significant for both deterministic ( $P[\theta \geq \theta_{obs}] = 0$ , N = 1000 randomization) and  
210 stochastic IPMs; there were also significant effects of IPM type, habitat, and their interaction on  $\lambda$   
211 (Table 4). Because stochasticity is predicted to reduce population growth rates (Tuljapurkar et al. 2003;  
212 Doak et al. 2005; Metcalf et al. 2015), we were surprised to find that deterministic  $\lambda$  was nearly identical  
213 to the average  $\lambda$  from standard Stochastic IPMs (i.e., without lagged effects, Figure 2). However, we did  
214 see reductions in population growth rate when including lagged effects in IPMs: on average the projections  
215 of  $\lambda$  from these models were 1.5-2% lower, with 70-76% of the values below deterministic  $\lambda$  (Figure 2). The  
216 IPMs with lagged effects also appear to be more accurate — the underlying vital rate models for IPMs  
217 with lagged effects all had the best fit to the survey data (dAIC = 0, Table 1).

218 Including lagged effects in IPMs also resulted in significantly less predictable projections of population  
219 structure, both within (Figure 3 A) and across habitats (Figure 3 B, Table 5). This variability is  
220 particularly notable in forest fragments (Figure 4, Table 6), where we have previously shown lagged effects  
221 have very large impacts on growth and survival (Scott et al. 2022). The deterministic IPM for Continuous  
222 Forest projected slightly more of the smallest and largest plants than the one for Forest Fragments. In  
223 other words, populations in forest fragments had proportionately less recruitment and fewer individuals  
224 growing into the larger, reproductive size classes (Bruna and Oli 2005). This shift towards intermediately  
225 sized, pre-reproductive plants in forest fragments is even more dramatic when using the stochastic IPM

226 with lagged effects (Figure 3 B).

227 What are the implications of these results for the use of IPMs to study plant demography? The first is  
228 that failing to include lagged effects in models could significantly underestimate the growth rate of  
229 populations. While relative differences in projections of  $\lambda$  may be sufficient for some tests of theory, the  
230 actual value of projections may be critical in conservation or management settings. For example, they  
231 could be used to identify which populations face the greatest risk of extinction (e.g.,  $\lambda = 0.99$  vs.  $\lambda = 1.01$ )  
232 or, because even small differences in  $\lambda$  can have major short-term consequences for population dynamics  
233 (e.g.,  $\lambda = 1.01$  vs.  $\lambda = 1.02$ ), be used to choose among alternative management strategies. Moreover,  
234 including lagged effects in models could be especially critical for studies assessing the effects of climate  
235 change, given many DLHE are climate driven.

236 The second implication is that demographic precision is computationally costly. While Deterministic  
237 IPMs and the Stochastic IPMs without lagged effects took only ~0.02 and ~0.07 min to iterate  
238 (respectively), the Stochastic IPMs including lags took ~87.12 min. This is largely due to the required  
239 computational resources and algorithms (i.e., `predict()`), which are much slower for Generalized Additive  
240 Models with 2D smooths than for the GAMs used in Deterministic and Stochastic IPMs. Advances in  
241 computational power and access to high-performance computing resources could lower this temporal and  
242 computational cost, as could GAMs for large datasets (i.e., Wood 2011). Until these resources are more  
243 broadly available, it is important to consider how failing to include lagged effects in demographic models  
244 could influence conclusions drawn from their analysis.

245 It is important to emphasize, however, that computational power cannot compensate for limited data.  
246 Detecting lagged effects and evaluating their consequences requires long-term demographic data — data  
247 that are only available for a relatively small number of species, few of which are in the tropics (Bruna et al.  
248 2009; Römer et al. 2024). The increasing evidence that lagged effects are ubiquitous, and that they can  
249 have major demographic impacts, underscores the need to support the collection of such long-term data,  
250 the complementary development of experimental and statistical approaches to disentangling lagged effects,  
251 and community driven efforts to identify priority or model systems for in-depth investigation.

## 252 Acknowledgments

253 We thank M. Acevedo, O. Acevedo-Charry, and \_\_\_\_\_ anonymous reviewers for helpful discussions and  
254 comments on the manuscript. We also thank Sam Levin for his help with the `ipmr` package. Financial  
255 support for collecting the demographic data used in this study was provided by the U.S. National Science  
256 Foundation (awards INT 98-06351, DEB-0309819, DEB-0614149, DEB-0614339, and DEB-1948607). This

257 article is publication no. \_\_\_\_ in the BDFFP Technical series. The authors declare no conflicts of interest.

258

## CRediT Statement

259 The authors made the following contributions: Eric R. Scott: conceptualization, methodology, formal  
260 analysis, validation, visualization, data curation, software, writing – original draft, review, and editing;  
261 Emilio M. Bruna: conceptualization, methodology, formal analysis, validation, visualization, data curation,  
262 software, writing (original draft, review and editing), funding acquisition, project administration,  
263 supervision; Maria Uriarte: conceptualization, methodology, writing (review and editing), funding  
264 acquisition.

265

## Data Availability Statement

266 Data and R code used in this study are archived with Zenodo at (*doi and url to be added on acceptance*).

267

## Literature Cited

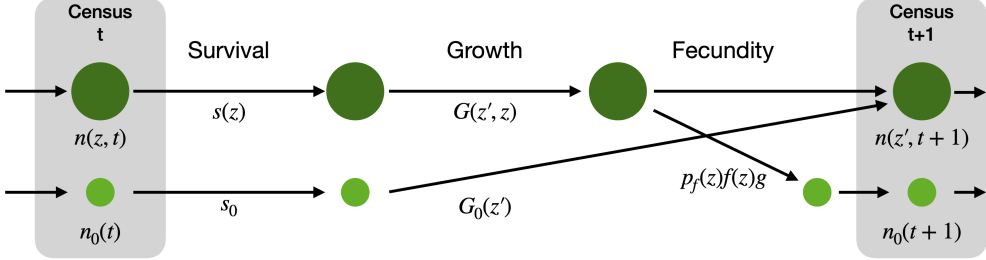
- 268 Beckerman, A., T. G. Benton, E. Ranta, V. Kaitala, and P. Lundberg. 2002. [Population dynamic](#)  
269 [consequences of delayed life-history effects](#). Trends in Ecology & Evolution 17:263–269.
- 270 Bierregaard, R. O., C. Gascon, T. E. Lovejoy, and R. Mesquita, eds. 2001. Lessons from Amazonia: The  
271 ecology and conservation of a fragmented forest. Yale University Press, New Haven.
- 272 Boyce, M., C. Haridas, C. Lee, and The Stochastic Demography Working Group. 2006. [Demography in an](#)  
273 [increasingly variable world](#). Trends in Ecology & Evolution 21:141–148.
- 274 Brooks, M. E., K. Kristensen, M. R. Darrigo, P. Rubim, M. Uriarte, E. M. Bruna, and B. M. Bolker. 2019.  
275 [Statistical modeling of patterns in annual reproductive rates](#). Ecology 100:e02706.
- 276 Bruna, E. M. 1999. [Seed germination in rainforest fragments](#). Nature 402:139.
- 277 ———. 2002. [Effects of forest fragmentation on \*Heliconia acuminata\* seedling recruitment in central](#)  
278 [Amazonia](#). Oecologia 132:235–243.
- 279 ———. 2003. [Are plant populations in fragmented habitats recruitment limited? Tests with an](#)  
280 [Amazonian herb](#). Ecology 84:932–947.
- 281 ———. 2014. [Dataset: \*Heliconia acuminata\* seed set \(seeds per fruit\)](#). Figshare doi:  
282 10.6084/m9.figshare.1273926.v2.
- 283 ———. 2021. [Dataset: Leaf number, leaf area, shoot number, and height of reproductive \*H. Acuminata\*](#).  
284 Zenodo <https://doi.org/10.5281/zenodo.5041931>.
- 285 Bruna, E. M., I. J. Fiske, and M. D. Trager. 2009. [Habitat fragmentation and plant populations: Is what](#)  
286 [we know demographically irrelevant?](#) Journal of Vegetation Science 20:569–576.
- 287 Bruna, E. M., and W. J. Kress. 2002. [Habitat fragmentation and the demographic structure of an](#)  
288 [Amazonian understory herb \(\*Heliconia acuminata\*\)](#). Conservation Biology 16:1256–1266.

- 289 Bruna, E. M., W. J. Kress, F. Marques, and O. F. da Silva. 2004. *Heliconia acuminata* reproductive  
290 success is independent of local floral density. *Acta Amazonica* 34:467–471.
- 291 Bruna, E. M., and M. K. Oli. 2005. Demographic effects of habitat fragmentation on a tropical herb:  
292 Life-table response experiments. *Ecology* 86:1816–1824.
- 293 Bruna, E. M., M. Uriarte, M. R. Darrigo, P. Rubim, C. F. Jurinitz, E. R. Scott, O. Ferreira da Silva, et al.  
294 2023. Demography of the understory herb *Heliconia acuminata* (Heliconiaceae) in an experimentally  
295 fragmented tropical landscape. *Ecology* 104:e4174.
- 296 Caswell, H. 2001. Matrix population models: Construction, analysis, and interpretation. Sinauer  
297 Associates, Sunderland.
- 298 Cosar, G., and O. Dag. 2024. Vartest: Tests for variance homogeneity. doi:  
299 [10.32614/CRAN.package.vartest](https://doi.org/10.32614/CRAN.package.vartest).
- 300 Criley, R., and S. Lekawatana. 1994. Year around production with high yields may be a possibility for  
301 *Heliconia chartacea*. *Acta Horticulturae* 397:95–102.
- 302 Crone, E. E., E. S. Menges, M. M. Ellis, T. Bell, P. Bierzychudek, J. Ehrlen, T. N. Kaye, et al. 2011. How  
303 do plant ecologists use matrix population models? *Ecology Letters* 14:1–8.
- 304 Doak, D. F., W. F. Morris, C. Pfister, B. E. Kendall, and E. M. Bruna. 2005. Correctly estimating how  
305 environmental stochasticity influences fitness and population growth. *The American Naturalist*  
306 166:E14–E21.
- 307 Ellner, S. P., D. Z. Childs, and M. Rees. 2016. Data-driven modelling of structured populations: A  
308 practical guide to the integral projection model. Springer Science+Business Media, New York, NY.
- 309 Ellner, S. P., and M. Rees. 2006. Integral projection models for species with complex demography.  
310 *American Naturalist* 167:410–428.
- 311 Evers, S. M., T. M. Knight, D. W. Inouye, T. E. X. Miller, R. Salguero-Gómez, A. M. Iler, and A.

- 312 Compagnoni. 2021. Lagged and dormant season climate better predict plant vital rates than climate  
313 during the growing season. Global Change Biology 27:1927–1941.
- 314 Kassambara, A. 2023. Rstatix: Pipe-friendly framework for basic statistical tests. doi:  
315 [10.32614/CRAN.package.rstatix](https://doi.org/10.32614/CRAN.package.rstatix).
- 316 Kress, J. 1990. The diversity and distribution of *Heliconia* (Heliconiaceae) in Brazil. Acta Botanica  
317 Brasileira 4:159–167.
- 318 Kress, W. J. 1983. Self-incompatibility systems in Central American *Heliconia*. Evolution 37:735–744.
- 319 Kuss, P., M. Rees, H. H. Ægisdóttir, S. P. Ellner, and J. Stöcklin. 2008. Evolutionary demography of  
320 long-lived monocarpic perennials: A time-lagged integral projection model. Journal of Ecology 96:821–832.
- 321 Landau, W. M. 2021. The targets R package: A dynamic Make-like function-oriented pipeline toolkit for  
322 reproducibility and high-performance computing. Journal of Open Source Software 6:2959.
- 323 Levin, S. C., D. Z. Childs, A. Compagnoni, S. Evers, T. M. Knight, and R. Salguero-Gómez. 2021. Ipmr:  
324 Flexible implementation of Integral Projection Models in R. Methods in Ecology and Evolution  
325 12:1826–1834.
- 326 Manly, B. F. 2018. Randomization, bootstrap and Monte Carlo methods in biology. Chapman and  
327 Hall/CRC, New York.
- 328 Metcalf, C. J. E., S. P. Ellner, D. Z. Childs, R. Salguero-Gómez, C. Merow, S. M. McMahon, E. Jongejans,  
329 et al. 2015. Statistical modelling of annual variation for inference on stochastic population dynamics using  
330 Integral Projection Models. Methods in Ecology and Evolution 6:1007–1017.
- 331 Molowny-Horas, R., M. L. Suarez, and F. Lloret. 2017. Changes in the natural dynamics of *Nothofagus*  
332 *Dombeyi* forests: Population modeling with increasing drought frequencies. Ecosphere 8:1–17.
- 333 Morris, W. F., and D. F. Doak. 2002. Quantitative conservation biology: Theory and practice of  
334 population viability analysis. Sinauer, Sunderland, MA.

- 335 R Core Team. 2020. [R: A language and environment for statistical computing](#). Vienna, Austria  
336 <https://www.R-project.org/>.
- 337 Rees, M., D. Z. Childs, and S. P. Ellner. 2014. [Building integral projection models: A user's guide](#). Journal  
338 of Animal Ecology 83:528–545.
- 339 Rees, M., and S. P. Ellner. 2009. [Integral projection models for populations in temporally varying](#)  
340 [environments](#). Ecological Monographs 79:575–594.
- 341 ———. 2016. [Evolving integral projection models: Evolutionary demography meets eco-evolutionary](#)  
342 [dynamics](#). Methods in Ecology and Evolution 7:157–170.
- 343 Ribeiro, M. B. N., E. M. Bruna, and W. Mantovani. 2010. [Influence of post-clearing treatment on the](#)  
344 [recovery of herbaceous plant communities in Amazonian secondary forests](#). Restoration Ecology 18:50–58.
- 345 Römer, G., J. P. Dahlgren, R. Salguero-Gómez, I. M. Stott, and O. R. Jones. 2024. [Plant demographic](#)  
346 [knowledge is biased towards short-term studies of temperate-region herbaceous perennials](#). Oikos  
347 2024:e10250.
- 348 Salguero-Gómez, R., O. R. Jones, C. R. Archer, Y. M. Buckley, J. Che-Castaldo, H. Caswell, D. Hodgson,  
349 et al. 2015. [The COMPADRE Plant Matrix Database: An open online repository for plant demography](#).  
350 Journal of Ecology 103:202–218.
- 351 Scott, E. R., M. Uriarte, and E. M. Bruna. 2022. [Delayed effects of climate on vital rates lead to](#)  
352 [demographic divergence in Amazonian forest fragments](#). Global Change Biology 28:463–479.
- 353 Stouffer, P. C., and R. O. Bierregaard. 1996. Forest fragmentation and seasonal patterns of hummingbird  
354 abundance in Amazonian Brazil. Ararajuba 4:9–14.
- 355 Tenhumberg, B., E. E. Crone, S. Ramula, and A. J. Tyre. 2018. [Time-lagged effects of weather on plant](#)  
356 [demography: Drought and \*Astragalus scaphoides\*](#). Ecology 99:915–925.
- 357 Tuljapurkar, S., C. C. Horvitz, and J. B. Pascarella. 2003. [The many growth rates and elasticities of](#)

- 358 populations in random environments. *The American Naturalist* 162:489–502.
- 359 Uriarte, M., M. Anciães, M. T. B. da Silva, R. Rubim, E. Johnson, and E. M. Bruna. 2011. Disentangling  
360 the drivers of reduced long-distance seed dispersal by birds in an experimentally fragmented landscape.  
361 *Ecology* 92:924–937.
- 362 Williams, J. L., H. Jacquemyn, B. M. Ochocki, R. Brys, T. E. X. Miller, and R. Shefferson. 2015. Life  
363 history evolution under climate change and its influence on the population dynamics of a long-lived plant.  
364 *Journal of Ecology* 103:798–808.
- 365 Williams, J. L., T. E. Miller, and S. P. Ellner. 2012. Avoiding unintentional eviction from integral  
366 projection models. *Ecology* 93:2008–2014.
- 367 Wood, S. N. 2011. Fast stable restricted maximum likelihood and marginal likelihood estimation of  
368 semiparametric generalized linear models. *Journal of the Royal Statistical Society Series B: Statistical  
369 Methodology* 73:3–36.
- 370 Xavier, A. C., C. W. King, and B. R. Scanlon. 2016. Daily gridded meteorological variables in Brazil  
371 (1980–2013). *International Journal of Climatology* 36:2644–2659.



Description	Deterministic	Stochastic, kernel-resampled	Stochastic, parameter-resampled
Survival	$s(z)$	$s_y(z)$	$s(z; \theta_{0-36})$
Growth	$G(z'; z)$	$G_y(z'; z)$	$G(z', z; \theta_{0-36})$
Flowering	$p_f(z)$	$p_{f_y}(z)$	$p_f(z; \theta_{0-36})$
Size-specific fecundity	$f(z)$	$f(z)$	$f(z)$
Germination & establishment	$g$	$g$	$g$
Seedling survival	$s_0$	$s_{0_y}$	$s_0(\theta_{0-36})$
Seedling growth	$G_0(z')$	$G_{0_y}(z')$	$G_0(z'; \theta_{0-36})$

**fig. 1.** Life cycle diagram of *Heliconia acuminata*. Each transition is associated with an equation for a vital rate function. The functions shown on the diagram correspond to those used to construct a general, density-independent, deterministic IPM. The table below shows the equivalent equations for stochastic IPMs with and without lagged effects (i.e., kernel-resampled vs. parameter-resampled IPMs).

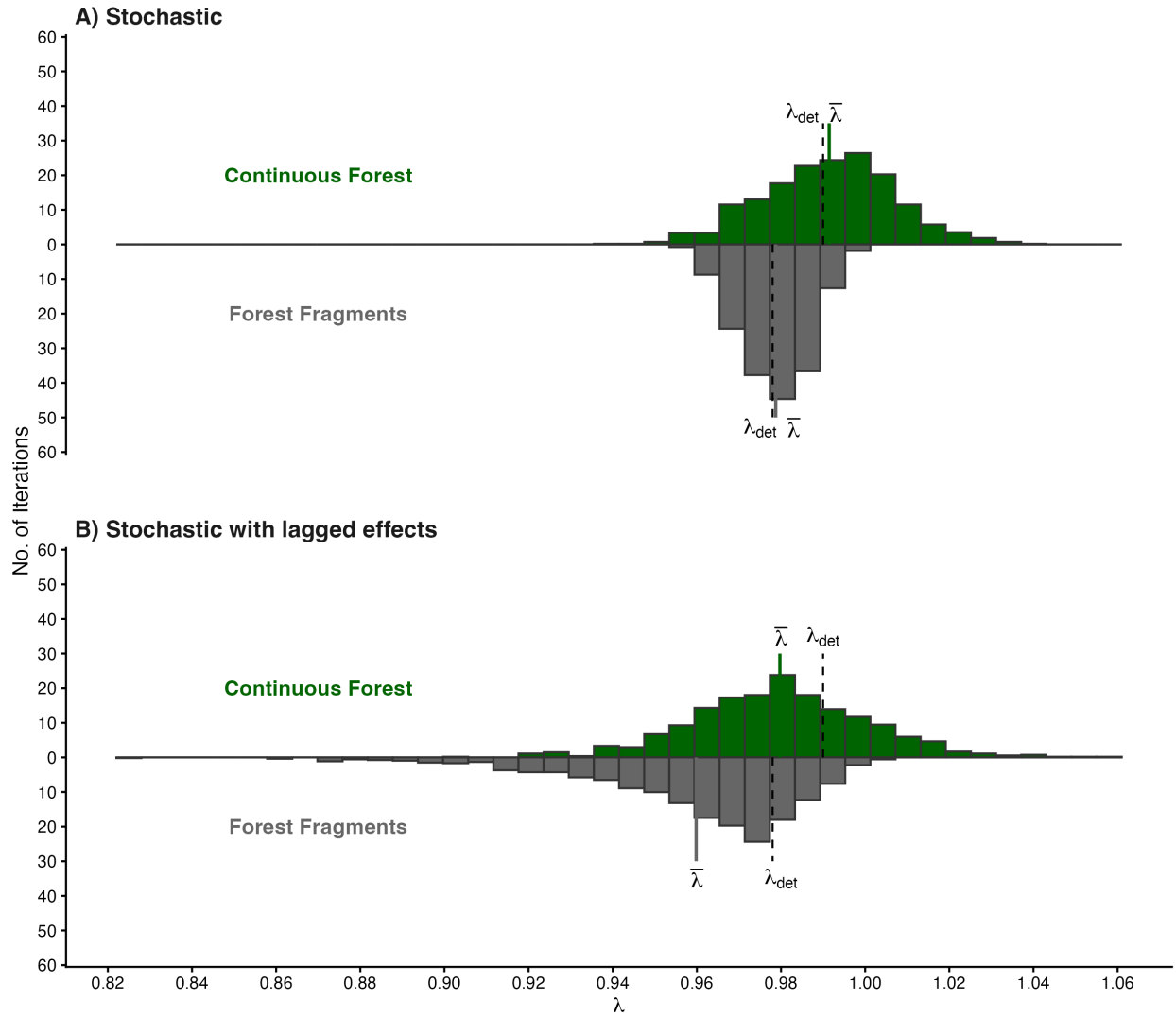


**fig. 2.** Distribution of 900 values of  $\lambda$  projected with (A) Stochastic IPMs without lagged effects and (B) Stochastic IPMs with lagged effects. IPMs were used to project  $\lambda$  for both Continuous Forest (above, in green) and Forest Fragments (below, in gray). The solid line indicates the mean value of  $\lambda$ , the dashed line indicates the value of  $\lambda$  in that habitat projected with Deterministic IPMs.

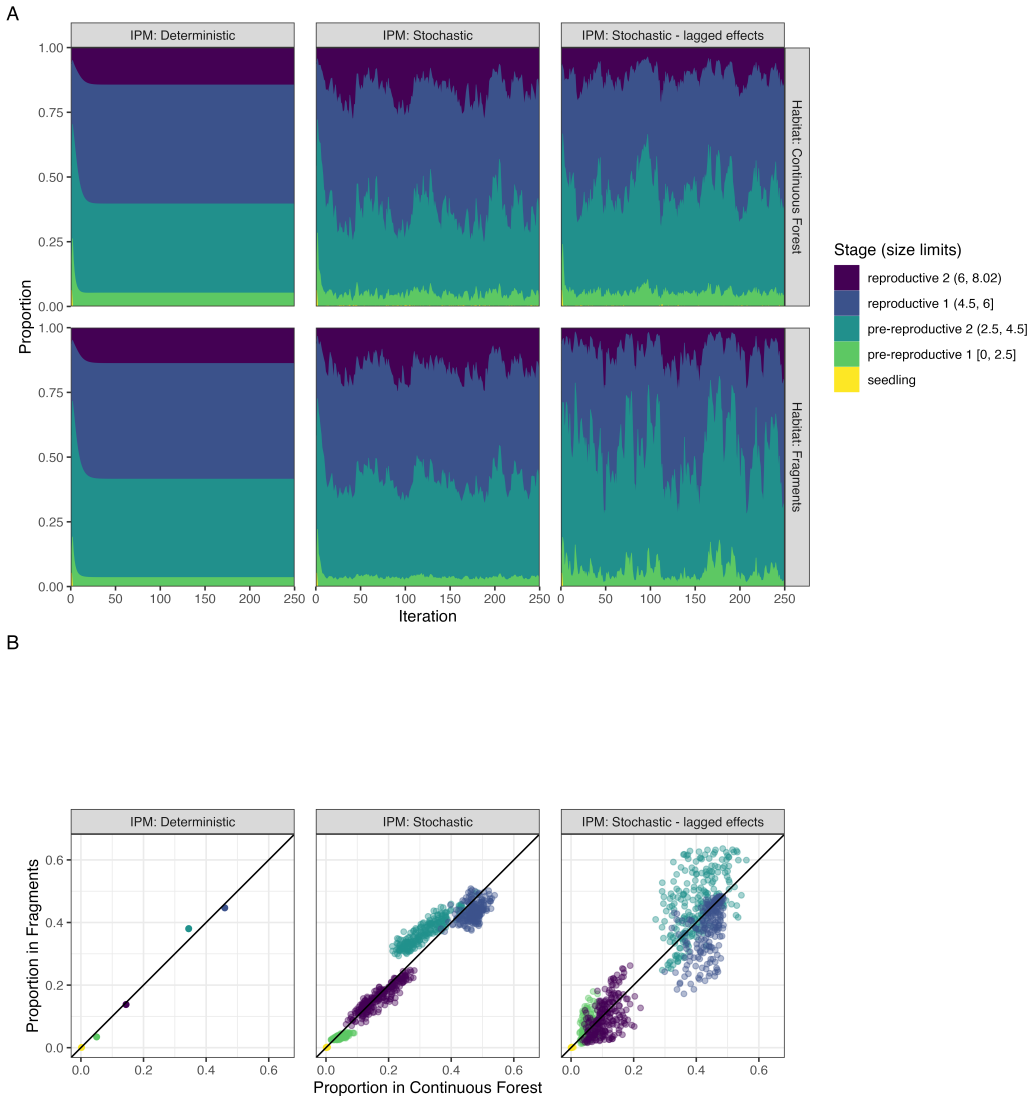


**fig. 3. (A)** The change over time in the the proportion of *Heliconia acuminata* populations in different size/stage classes when simulating population dyammics in Continuous Forest (CF) or Forest Fragment (FF) with three different integral projection models (e.g., IPMs). Results are shown for the first 250 iterations of populations; for the criteria used to define the size categories see Table 2. **(B)** The relative proportion of the population in each size class (FF vs. CF) for 250 iterations of each IPM model. Note that this excludes transient dynamics (iterations 1-30). Values on the 1-1 line indicate an iteration where CF and FF have the same proportion of the population in a given size class.

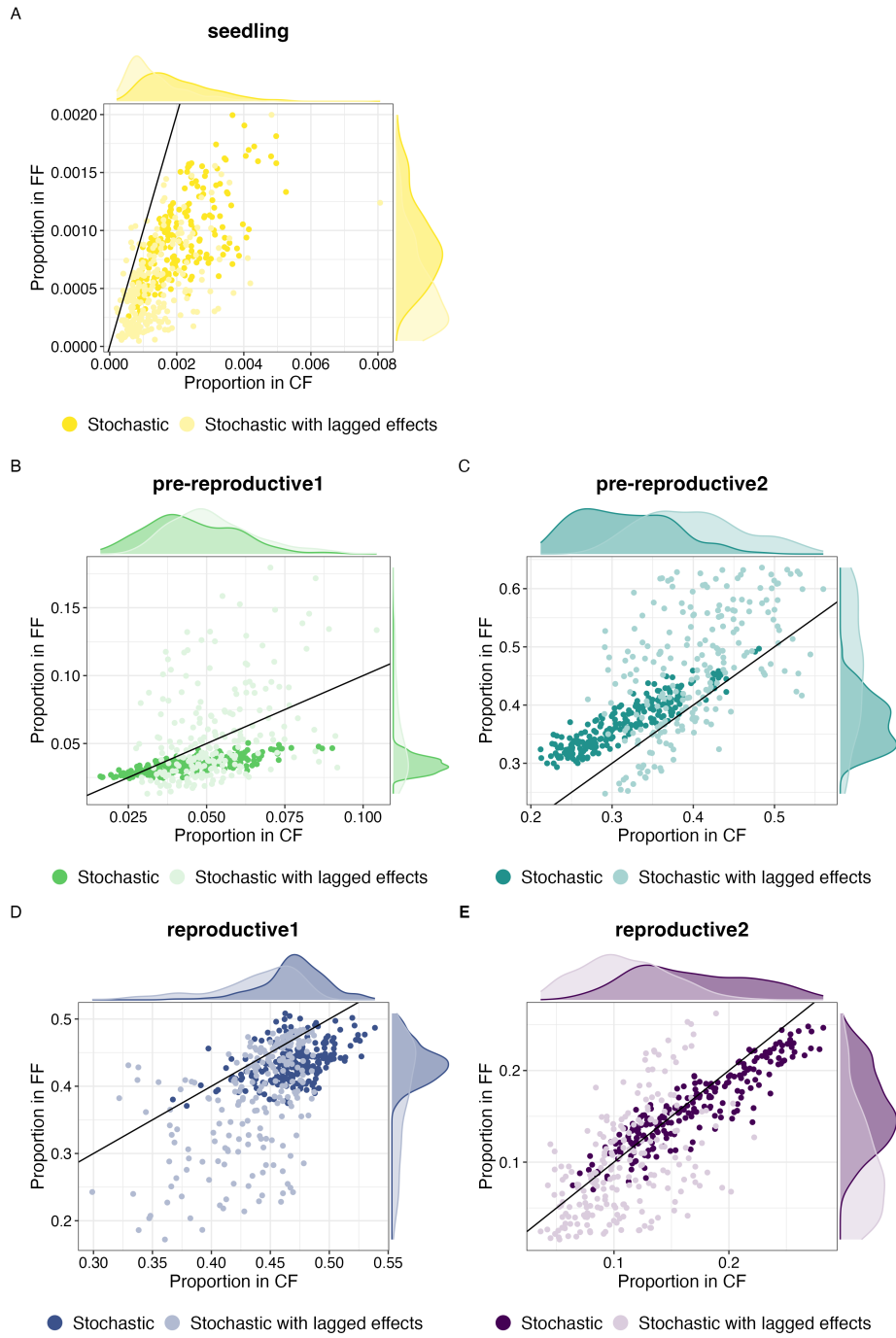


**fig. 4.** The relative proportion of the population in each size class (FF vs. CF) for each of 250 iterations of the no-lag IPMs (dark shading) and Stochastic IPMs with lagged effects (light shading). Values on the 1-1 line indicate an iteration where CF and FF have the same proportion of the population in a given size class; the marginal plots indicate the distribution of these relative proportions for each class of IPM in each habitat. Note that both the scatterplots and marginal plots exclude transient dynamics (iterations 1-30).

Table 1: Comparison of vital rate models used to build IPM. The ‘Effect of Environment’ column describes how environmental effects were included in models. Those with ‘none’ were used to build deterministic IPMs; those with a random effect of year were used to build stochastic IPMs without lagged effects (i.e., kernel-resampled models); and those with a distributed lag non-linear model (DLNM) were used to build stochastic IPMs with lagged effects (i.e., parameter-resampled models). ‘edf’ is the estimated degrees of freedom of the penalized GAM.  $\Delta\text{AIC}$  is calculated within each habitat and vital rate combination.  $\Delta\text{AIC}$  within 2 indicates models are equivalent.

Habitat	Vital Rate	Effect of Environment	<i>edf</i>	$\Delta\text{AIC}$
<b>Continuous Forest</b>				
	Survival	Random effect of year	43.26	0.00
		DLNM	19.72	78.92
		None	4.98	260.01
	Growth	Random effect of year	78.43	0.00
		DLNM	23.87	158.46
		None	7.81	1896.03
	Flowering	DLNM	19.59	0.00
		Random effect of year	17.19	1.63
		None	7.47	381.86
	Seedling survival	None	1.00	0.00
		Random effect of year	1.82	1.39
		DLNM	4.01	1.53
	Seedling growth	Random effect of year	9.47	0.00
		DLNM	8.95	2.90
		None	1.00	172.33
<b>Forest Fragments</b>				
	Survival	DLNM	14.95	0.00
		Random effect of year	19.21	35.68
		None	4.33	51.25
	Growth	DLNM	25.18	0.00
		Random effect of year	37.84	199.98
		None	5.60	382.76
	Flowering	DLNM	20.61	0.00
		Random effect of year	13.81	27.40
		None	5.01	101.70
	Seedling survival	DLNM	5.57	0.00
		Random effect of year	5.09	5.72
		None	1.00	6.49
	Seedling growth	Random effect of year	6.25	0.00
		DLNM	8.18	2.29
		None	1.00	5.74

Table 2: Size and stage categories used for comparing *Heliconia acuminata* population structure. Note that seedlings are a discrete size class not based on size (see *Methods* for additional details).

Category	Log(size)	Avg. prob. survival	Prob. flowering
Seedlings	-	-	-
Pre-reproductive 1	0–2.5	$\leq 0.9$	$\approx 0$
Pre-reproductive 2	2.5–4.5	$\geq 0.8$	$\approx 0$
Reproductive 1	4.5–6	$\geq 0.95$	$\leq 0.25$
Reproductive 2	$\geq 6$	$\geq 0.95$	$\geq 0.2$

Table 3: Population growth rates for continuous forest (CF) and forest fragments (FF) under different kinds of IPMs with bootstrapped, bias-corrected, 95% confidence intervals.

IPM	Habitat	$\lambda$	95% CI (Lower, Upper)
<b>Deterministic</b>			
	FF	0.9778	(0.9736, 0.9823)
	CF	0.9897	(0.9877, 0.9920)
<b>Stochastic</b>			
	FF	0.9787	(0.9735, 0.9835)
	CF	0.9913	(0.9892, 0.9939)
<b>Stochastic with lagged effects</b>			
	FF	0.9595	(0.9459, 0.9689)
	CF	0.9795	(0.9752, 0.9867)

Table 4: Estimated parameters, standard errors, t-values and P-values for the GLM of the effect of Habitat and IPM Type on projections of lambda.

Term	Estimate	SE	z value	P
(Intercept)	0.98	0	1568.20	< 0.0001
$Habitat_{FF}$	-0.02	0	-22.52	< 0.0001
$IPM_{Stoch}$	0.01	0	13.27	< 0.0001
$Habitat_{FF} : IPM_{Stoch}$	0.01	0	5.76	< 0.0001

Table 5: Results of statistical tests comparing the variance in the proportion of each habitat's population projected to be in each stage class by Stochastic IPMs with and without lagged effects ( $N = 220$  projections per stage class). The variances for each habitat  $\times$  stage class  $\times$  IPM combination can be found in Table 6. Comparisons where the p-value of the test was  $< 0.05$  are indicated with an asterisk.

Stage	Habitat	Statistic	<i>df</i>	<i>P</i>
<b>Seedling</b>				
	CF	4.59	1	0.032*
	FF	11.51	1	0.001*
<b>Pre-reproductive 1</b>				
	CF	8.73	1	0.003*
	FF	96.13	1	< 0.0001*
<b>Pre-reproductive 2</b>				
	CF	0.99	1	0.319
	FF	39.67	1	< 0.0001*
<b>Reproductive 1</b>				
	CF	0.57	1	0.452
	FF	61.58	1	< 0.0001*
<b>Reproductive 2</b>				
	CF	0.11	1	0.745
	FF	18.78	1	< 0.0001*

Table 6: Summary statistics (median, mean, and variance) describing the proportion of populations projected to be in each of five life-history stages by Stochastic IPMs with and without lagged effects (i.e., kernel- vs. parameter-resampled IPMs, N = 220 projections for each IPM class x habitat combination.)

Stage	IPM	Median		Mean		Variance	
		CF	FF	CF	FF	CF	FF
<b>Seedling</b>							
	Stochastic	0.0018	0.0009	0.0020	0.0020	0.000001	0.000000
	Stochastic with lagged effects	0.0011	0.0004	0.0014	0.0014	0.000001	0.000000
<b>Pre-reproductive 1</b>							
	Stochastic	0.0426	0.0340	0.0450	0.0450	0.000203	0.000034
	Stochastic with lagged effects	0.0499	0.0438	0.0522	0.0522	0.000192	0.001167
<b>Pre-reproductive 2</b>							
	Stochastic	0.3097	0.3677	0.3147	0.3147	0.003354	0.001884
	Stochastic with lagged effects	0.3975	0.4613	0.4002	0.4002	0.003934	0.010380
<b>Reproductive 1</b>							
	Stochastic	0.4725	0.4332	0.4704	0.4704	0.000736	0.000822
	Stochastic with lagged effects	0.4464	0.4049	0.4371	0.4371	0.001481	0.006388
<b>Reproductive 2</b>							
	Stochastic	0.1630	0.1554	0.1679	0.1679	0.002630	0.001745
	Stochastic with lagged effects	0.1062	0.0882	0.1092	0.1092	0.001427	0.003213